NJC

ROYAL SOCIETY OF CHEMISTRY

PAPER

View Article Online
View Journal | View Issue

Cite this: *New J. Chem.*, 2021, 45, 9462

Highly efficient diglycolamide-functionalized dendrimers for the sequestration of tetravalent actinides: solvent extraction and theoretical studies†

Parveen K. Verma, [a] Rajesh B. Gujar,[a] Prasanta K. Mohapatra, *[a] Sk. Musharaf Ali, [b] Andrea Leoncini,[c] Jurriaan Huskens [c] and Willem Verboom *[c]

Received 11th February 2021,
Accepted 16th April 2021

DOI: 10.1039/d1nj00724f

rsc.li/njc

Two diglycolamide (DGA) functionalized poly(propylene imine)diaminobutane dendrimers, first generation (Gen I) and second generation (Gen II), termed as $\mathbf{L_I}$ and $\mathbf{L_{II}}$, were used for the extraction of the tetravalent actinide ions Np^{4+} and Pu^{4+} from nitric acid medium. The metal ion extraction followed a 'solvation' type mechanism showing increasing metal ion extraction with increasing nitric acid concentration with species of the type: $M(NO_3)_4{\cdot}L$ (M = Np or Pu) with some contribution of $M(NO_3)_4{\cdot}2L$ for Pu. Pu^{4+} formed much stronger complexes with both DGA-dendrimer ligands as compared with Np^{4+}, as reflected in their two-phase extraction constants and higher ΔH values, attributed to its higher ionic potential. Binding of the metal ions was to one 'DGA pocket' in each of the dendrimers. The structure and bonding analysis was done on the basis of DFT studies.

Introduction

Diglycolamides are reported to be the most efficient extractants[1] for 'Actinide Partitioning'[2] which is considered relevant at the back end of the nuclear fuel cycle for the management of high level liquid waste (HLLW).[3] TODGA (*N*,*N*,*N*′,*N*′-tetra-*n*-octyl diglycolamide), the most studied diglycolamide (DGA) ligand,[4] extracts trivalent actinide ions such as Am^{3+} from moderate concentrations of nitric acid (3–4 M) to a much greater extent than the UO_2^{2+} ion, underlining its utility in HLLW management as compared with previously known and well studied ligands such as CMPO (carbamoylmethyl phosphine oxide),[5] DIDPA (diisodecylphosphoric acid),[6] TRPO (trialkylphosphine oxide)[7] and even malonamides such as DMDOHEMA (*N*,*N*′-dimethyl-*N*,*N*′-dioctylhexylethoxy malonamide)[8] which extracts the UO_2^{2+} ion to a much larger extent than the Am^{3+} ion. In view of the higher potential of TODGA for the extraction of minor actinide ions such as Am^{3+}, several of 'hot' counter-current extraction studies have been performed by various research groups.[9]

Recently, attempts have been made to synthesize ligands with multiple DGA groups where DGA moieties have been grafted to suitable scaffolds such as calix[4]arene,[10] pillar[5]arene,[11] TREN-based tripodals[12] or even a planar scaffold such as benzene.[13] We have recently reported poly(propylene imine) diaminobutane dendrimers containing DGA groups with very interesting results where the distribution ratio (D) values for Am^{3+} ion with the generation zero (Gen 0) dendrimer ($D \approx 0.1$) increased by over 2 and 3 orders of magnitude when Gen I and Gen II dendrimers ($\mathbf{L_I}$ and $\mathbf{L_{II}}$, respectively; Fig. 1) were used under identical conditions.[14] However, apart from our results on the extraction of the Am^{3+} ion, these DGA-functionalized dendrimers have been practically unexplored for the extraction of other important actinides present in HLLW.

Sasaki *et al.*, in their first paper on the extraction of actinide using TODGA, reported a much larger extraction of Np^{4+} and Pu^{4+} than that of Am^{3+}.[4a] It is understood that Pu produced during reactor operations (major constituent: ^{239}Pu; $t_{1/2}$: 24 100 year) exists in a quite significant concentrations in the HLLW from PUREX (Plutonium Uranium Redox Extraction) losses. Similarly, the concentration of Np, another activation product, in the HLLW of PWR origin (burn up: 33 000 MWd per T) is *ca.* 0.067 mg g^{-1},[15] which is mainly due to ^{237}Np ($t_{1/2}$: 2.1×10^6 year). As per the 'Actinide Partitioning' scheme of safe management of HLLW, it is required to separate the long-lived radionuclides such

[a] *Radiochemistry Division, Bhabha Atomic Research Centre, Mumbai 400 085, India. E-mail: mpatra@barc.gov.in*
[b] *Chemical Engineering Division, Bhabha Atomic Research Centre, Mumbai 400 085, India*
[c] *Laboratory of Molecular Nanofabrication, MESA + Institute for Nanotechnology, University of Twente, P.O. Box 217, 7500 AE Enschede, The Netherlands. E-mail: w.verboom@utwente.nl*

† Electronic supplementary information (ESI) available: Oxidation state adjustment; derivation extraction equilibrium constant; DFT data. See DOI: 10.1039/d1nj00724f

as Pu and Np from the HLLW for their subsequent transmutation in high flux reactors or in accelerator driven sub-critical system (ADSS).[16] Apart from this, ^{237}Np, if recovered from the HLLW can be used for the production of ^{238}Pu (power density: 0.57 Watt g^{-1})[17] by neutron activation for its application in power sources. In view of these facts, it is of great relevance to study the extraction behaviour of Np^{4+} and Pu^{4+} ions using highly efficient multiple DGA extractants such as the DGA-functionalized dendrimers $\mathbf{L_I}$ and $\mathbf{L_{II}}$. To our knowledge, so far there is no report available on the extraction of Pu^{4+} and Np^{4+} using these DGA-functionalized dendrimers.

Our previous studies on the complexation of trivalent lanthanide/actinide ions with these ligands suggested unusual binding with the ML_2 type of species, which cannot be easily explained on the basis of the coordination of DGA groups from two ligands. There was an issue of isolating the complexes due to the formation of pasty masses with the dendrimer ligands. Moreover, with their Np and Pu complexes, which have very high specific activities, it was not possible to work due to the large radioactivity associated with the complexes. Therefore, it was thought of interest to investigate the bonding of the tetravalent metal ions with the DGA-functionalized dendrimers $\mathbf{L_I}$ and $\mathbf{L_{II}}$ by DFT computational studies.

The present study involves the extraction of Np^{4+} and Pu^{4+} ions using the Gen I and Gen II DGA-functionalized dendrimers $\mathbf{L_I}$ and $\mathbf{L_{II}}$. After obtaining the nature of the extracted species by solvent extraction, an attempt was made to understand the bonding of the complexes with the DGA groups by DFT. The studies also include the determination of thermodynamic parameters for getting an idea about the extraction/complexation process.

Results and discussion

Solvent extraction studies

The DGA-functionalized poly(propylene imine) diaminobutane dendrimers $\mathbf{L_I}$ (Gen I) and $\mathbf{L_{II}}$ (Gen II) (Fig. 1) were evaluated for the solvent extraction of the tetravalent actinides Np(IV) and Pu(IV) from dilute to moderate nitric acid solutions. The extraction studies were carried out with 0.1 mM ligand in 5% IDA (isodecanol) + *n*-dodecane diluent due to the poor solubility of these ligands in pure *n*-dodecane.[1]

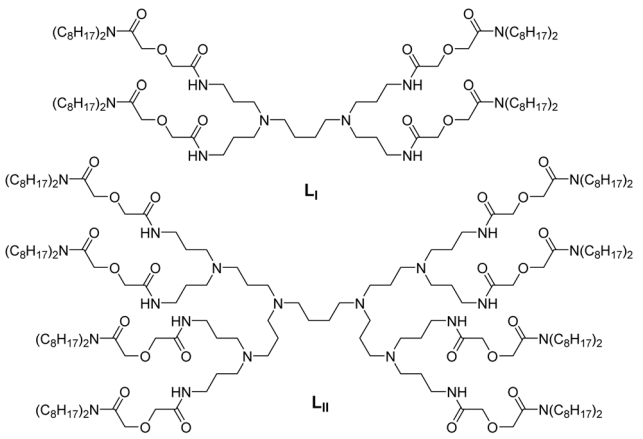

Fig. 1 Structure of the diglycolamide (DGA) functionalized poly(propylene imine) diaminobutane dendrimers, generation 1 ($\mathbf{L_I}$) and generation 2 ($\mathbf{L_{II}}$).

The uptake of water and nitric acid was studied both in the absence and the presence of the extractants. The results indicated about 1% extraction of the acid by the solvent (diluent + ligand) (Table S1, ESI†). The extraction of nitric acid by alcohols is well known[18] and the extracted acid forms the (extractant·nitric acid) complex as per the following equilibrium reaction.

$$x\mathrm{HNO_{3,aq}} + y\mathrm{L_{org}} \overset{K_H}{\rightleftharpoons} (\mathrm{HNO_3})_x{\cdot}y\mathrm{L_{org}} \qquad (1)$$

An attempt was made to determine the K_H values for both $\mathbf{L_I}$ and $\mathbf{L_{II}}$. The acid–base titration studies were not very conclusive due to the very small changes obtained with the ligand solutions *vis-à-vis* the blank (diluent mixture) as the changes were less than the experimental errors (Fig. S2; ESI†). On the other hand, FT-IR measurements clearly showed a shift in the carbonyl band of the ligand solutions after equilibration with 3 M HNO_3 (Fig. S3 and S4; ESI†). The K_H values were, therefore, obtained using the FTIR data (details are given in the ESI†) and were found to be 0.27 ($\pm$0.05) and 0.32 ($\pm$0.06) for $\mathbf{L_I}$ and $\mathbf{L_{II}}$, respectively which were very close to the reported values for other DGA ligands.[19,20]

The presence of 5% iso-decanol in the diluent mixture was responsible for the extraction of 0.05% (*ca.* 27.8 mM) of water into the organic phase as well (Table S1, ESI†) and might make the metal ions highly hydrated (in view of the tracer concentrations involved resulting in very high water to metal ion ratios) unless the DGA groups can replace them by strong complex formation (*vide infra*).

The extraction of both the tetravalent metal ions was fast with both the ligands in this diluent and the extraction equilibrium was attained in 15–20 minutes (Fig. S1; ESI†). We have also observed fast extraction kinetics for the trivalent actinides using the same ligand system.[14]

The extraction of both Np(IV) and Pu(IV) was also studied as a function of the feed acidity from 0.5 M to 6 M HNO_3. Acid concentrations $<$0.5 M were not used as the metal ions can be hydrolyzed.[21] The extraction of Np(IV)/Pu(IV) increased with the increase in the feed acidity for both ligands (Fig. 2a). The extraction of both the metal ions was found to be highly efficient as *ca.* 90% or higher extraction was observed even with 1×10^{-4} M ligand solutions. When compared with the extraction of the Am^{3+} ion,[14] the extraction of Pu^{4+} is comparable, albeit, with almost 10 times lower concentration of the ligands. Also, while using a 10 μM solution of the ligand $\mathbf{L_{II}}$, $>$90% extraction of Pu(IV) was possible. This suggests that the DGA-based dendrimer ligands $\mathbf{L_I}$ and $\mathbf{L_{II}}$ are highly promising for applications in radioactive waste management.

The general equilibrium for the extraction of M(IV) with L ($\mathbf{L_I}$/$\mathbf{L_{II}}$) in 5% IDA + *n*-dodecane can be written as eqn (2):

$$\mathrm{M^{4+}_{aq}} + a\mathrm{L_{f,org}} + b\mathrm{NO_3^-{}_{aq}} \overset{K_{ex}}{\rightleftharpoons} \mathrm{M(NO_3)}_b{\cdot}a\mathrm{L_{org}} \qquad (2)$$

where M is Np(IV)/Pu(IV), $L_{f,org}$ is the 'free' form (which does not exist as the (extractant·nitric acid) complex) of either $\mathbf{L_I}$ or $\mathbf{L_{II}}$ and

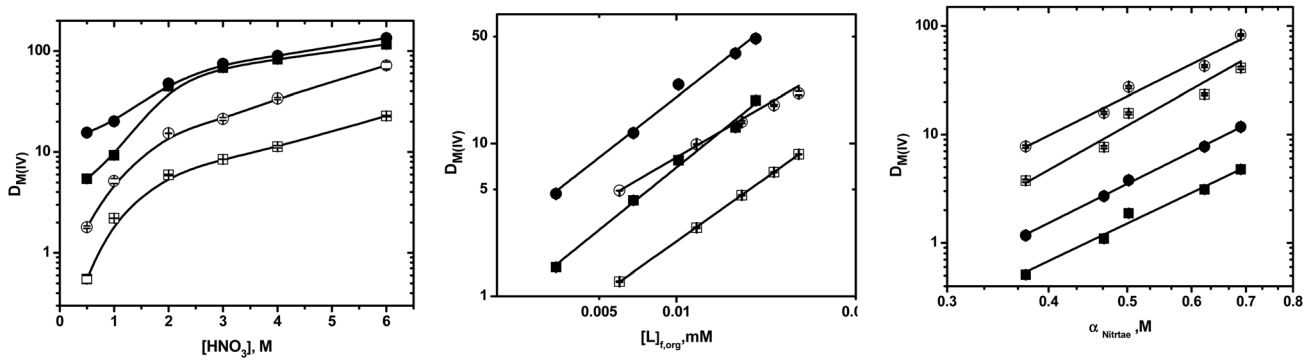

Fig. 2 The extraction of Np(IV) (open symbols) and Pu(IV) (closed symbols) as a function of (left) varying acidity using 1×10^{-4} M ligand solutions; (center) varying ligand concentration at 3 M HNO_3 and (right) varying nitrate ion concentration using 1×10^{-4} M ligand solutions. $\mathbf{L_I}$ (square) and $\mathbf{L_{II}}$ (circle) dissolved in 5% IDA+ *n*-dodecane; *T*: 298 K.

K_{ex} is the two-phase extraction constant. The subscripts 'aq' and 'org' indicate the species present in the aqueous and organic phases, respectively. The K_H values of the ligands, as mentioned above, were used to calculate the $L_{f,org}$ concentrations. Although an increase in the $D_{M(IV)}$ was observed for both ligands, the relative change in the $D_{M(IV)}$ differed depending on the ligand. The Np(IV) extraction showed a steady increase with the aqueous phase acidity. The extraction of the metal ions involves the replacement of the coordinated water molecules from the inner-sphere with the DGA groups. The extraction by the DGA-dendrimer $\mathbf{L_{II}}$ remained superior to that of $\mathbf{L_I}$ over the whole acidity range, whereas for the Pu(IV) extraction the change in the $D_{Pu(IV)}$ with different ligands was appreciable at lower acidity and merges at higher acidity. The higher extraction by $\mathbf{L_{II}}$ can either be attributed to the higher number of coordinating sites available for complexation or may be due to the higher lipophilicity of the extracted M(IV)–$\mathbf{L_{II}}$ complex compared with the M(IV)–$\mathbf{L_I}$ complex. The steady increase in the $D_{M(IV)}$ with the aqueous feed acidity suggest the solvation mechanism for the extraction of the tetravalent actinides with both ligands in 5% IDA + *n*-dodecane (Fig. 2a).

The extraction equilibrium constant for the present system can be given by eqn (3):

$$K_{ex} = \frac{\left[M(NO_3)_b \cdot aL\right]_{org}}{[M^{4+}]_{aq}[NO_3]^b_{aq}[L]^a_{f,org} \cdot \gamma_{M^{4+}} \cdot \gamma^b_{NO_3} \cdot \gamma^a_L} \quad (3)$$

where the square brackets represent the concentration of each species therein and γ is the activity coefficient for the given species. Assuming the activity constant for various species remains constant for the given concentration of L and NO_3^-, and its temperature dependence is very small, we can write eqn (4), obtained under the above assumptions:

$$K_{ex} = \frac{\left[M(NO_3)_b \cdot aL\right]_{org}}{[M^{4+}]_{aq}[NO_3]^b_{aq}[L]^a_{f,org}} \quad (4)$$

After a series of mathematical manipulations and approximations (ESI†), one can obtain the linearized form of the equation, containing the apparent extraction equilibrium constant (K'_{ex}), as:

$$\log D_M = \log K'_{ex} + a\log[L]_{f,org} + b\log[NO_3^-]_{aq} \quad (5)$$

where K'_{ex} is defined as the ratio of K_{ex} to K_{Nit} (the constant containing the nitrate ion complexation part; ESI†).

Eqn (5) gives the linear dependence of $\log D_M$ with the nitrate ion and ligand concentrations at a given temperature. All experiments were carried out at 298 K for the sake of convenience. The stoichiometry of the extracted complex in the organic phase can be found if the values of '*a*' and '*b*' are known from eqn (5). The values of '*a*' and '*b*' can easily be determined by evaluating D_M at varying concentrations of the free ligand in the organic phase at a fixed nitrate ion concentration and *vice versa*.

Stoichiometry of the extracted species

The stoichiometry of the extracted complexes in the solvent extraction of tetravalent actinides by $\mathbf{L_I}$/$\mathbf{L_{II}}$ in 5% IDA + *n*-dodecane was determined by the conventional slope analysis method.[14,22] To obtain the value of '*a*' from eqn (5), the concentration of the ligands ($\mathbf{L_I}$ or $\mathbf{L_{II}}$) was varied at a fixed acidity, *i.e.* 3 M HNO_3, and the distribution ratio values of Np(IV) and Pu(IV) were measured. The equilibrium free ligand concentration was assumed to be equal to the initial free ligand concentration as the amount of ligand involved in the complexation is very small due to very small concentrations of the metal ions used in the present study ([Np]: 10^{-12} M and [Pu]: 10^{-6} M). The $\log D_{M(IV)}$ *vs.* $\log[L]_{f,org}$ (L: $\mathbf{L_I}$/$\mathbf{L_{II}}$) gives average slope values of 1.20 ± 0.17 for all the systems (Fig. 2b) suggesting the involvement of one ligand in the extracted species. The slope values for the individual systems are given in Table S2 (ESI†). However, while the extracted species for Np(IV) resulted in slope values very close to 1, those for Pu(IV) yielded slopes close to 1.3, suggesting predominantly ML-type species with some contributions of ML_2. Similarly, the nitrate ion concentration variation experiments were done at a fixed HNO_3 concentration of 0.5 M (in order to prevent hydrolysis of the metal ions)[21] at a fixed ligand concentration (Fig. 2c). Since the concentration of the $NaNO_3$ used in the nitrate ion concentration variation experiments is large (0.5–3 M $NaNO_3$), the activities of the NO_3^- ($a(NO_3^-)$) ions were calculated using the activity coefficient

reported in literature and used for the $\log a(NO_3^-)$ calculations.[23,24] $\log D_{M(IV)}$ *vs.* $\log a(NO_3^-)$ plots were obtained for all the studied systems. Slope analysis of the linear log–log plot gives an average value of 3.70 ± 0.08 for all the systems, suggesting extraction of neutral $M(NO_3)_4L$ (L: $\mathbf{L_I}$ or $\mathbf{L_{II}}$) species for both the tetravalent metal ions by $\mathbf{L_I}$ or $\mathbf{L_{II}}$ dissolved in 5% IDA + *n*-dodecane (Fig. 2c). The formation of a similar neutral complex of type $Ln(III)(NO_3)_3L$ (L = $\mathbf{L_I}$ or $\mathbf{L_{II}}$), was also obtained for the extraction of trivalent metal ions by these ligands. Although, it can be expected, that the higher number of DGA arms in $\mathbf{L_{II}}$ can bind more metal ions giving a higher M : L ratio. However, the slope variation experiments suggested the formation of 1 : 1 M : L ratio complexes in the solvent extraction. The extraction of higher M : L complexes, such as 2 : 1 or higher, may be hindered due to the poor solubility of such polar complexes, with eight NO_3^- ions (to maintain neutrality) in the 2 : 1 complex, in the marginally polar 5% IDA + *n*-dodecane medium.[21]

Thermodynamic parameters of extraction

The extraction of the M(IV) by $\mathbf{L_I}$/$\mathbf{L_{II}}$ dissolved in 5% IDA + *n*-dodecane was studied at different temperatures to understand the thermodynamics of the extraction process. The extraction of Pu(IV) and Np(IV) was carried out at 1×10^{-5} M and 1×10^{-4} M $\mathbf{L_I}$/$\mathbf{L_{II}}$ in 5% IDA+ *n*-dodecane, respectively. This was required to obtain reasonably good *D* values for Pu(IV), as the values were very high with 1×10^{-4} M $\mathbf{L_I}$/$\mathbf{L_{II}}$. The *D* values for both Np(IV) and Pu(IV) were found to decrease with increasing temperature, suggesting the exothermic nature of the extraction process (Fig. 3). The activity coefficient values for all the species in eqn (2) were assumed to be unity, except for NO_3^- ions, due to the very small concentrations of the ligands ($\leq 10^{-4}$ M) and the metal ions ([Np]: 10^{-12} M and [Pu]: 10^{-6} M).[23–25] Assuming that the activity of NO_3^- and the free ligands remains unchanged with the varying temperature and the value of K_{Nit} (eqn (S5) in ESI†) also does not change significantly under the studied temperature range, eqn (6) (the Gibbs–Helmholtz equation and $\Delta G = -RT\ln K_{ex}'$) can be used to calculate the enthalpy change (ΔH) in the extraction of M(IV) by the different ligands at 3 M HNO_3.[22,26–28]

$$\log K_{ex}' = -(\Delta H_O/2.303R)(1000/T) + (\Delta S_O/2.303R) \quad (6)$$

The $\log K_{ex}'$ *vs.* $1/T$ plot gives a straight line, and the slope values were used to calculate the ΔH values (in kJ mol^{-1}) using eqn (7):

$$\Delta H_O = -2.303R \times \text{slope} \quad (7)$$

where R is the universal gas constant. The slope values are included in Table S2 (ESI†) and which can be used for the calculation of ΔH_O.

The values of K_{ex} for the extraction of M(IV) by $\mathbf{L_I}$/$\mathbf{L_{II}}$ were calculated at 3 M HNO_3 as mentioned in the ESI† (using eqn (S4)). For the computation of K_{ex}', the value of K_{Nit} was taken as 40.5 and 105 for Np(IV) and Pu(IV), respectively, at 3 M HNO_3.[29–31] The value of 2.78 was used for the $[NO_3^-]$, calculated using a K_a value of 23 for the dissociation of HNO_3.[28] The values of the thermodynamic parameters ΔG, ΔH_O and $T\Delta S$ were calculated as mentioned above. These values, together with the K_{ex}' values, are summarized in Table 1.

The overall enthalpy change (ΔH_O) during the solvent extraction of the tetravalent actinides can be viewed as the sum of the enthalpies of the different processes such as dehydration of the actinides (ΔH_W), complexation of the actinides with the ligands (ΔH_C) and dissolution of the neutral $M(NO_3)_4$·L complex into the molecular solvent (ΔH_D). The overall magnitude and the sign of ΔH_O depends on the contributions of all three, *i.e.* the ΔH_W, ΔH_C and ΔH_D terms.

$$\Delta H_O = \Delta H_W + \Delta H_D + \Delta H_C \quad (8)$$

Although the ΔH_W term may be positive (an endothermic process) for the dehydration of both Pu(IV) and Np(IV) as it is an energy intensive process, it may be more positive for the former because of its high ionic potential. The higher positive value of ΔH_W for Pu(IV) may be compensated by its higher negative value of ΔH_C compared with Np(IV). The ΔH_D values for the dissolution of the neutral $M(NO_3)_4$·L complexes must be very similar as the size of the complexes formed is predominantly decided by the size and number of associated ligands, which are the same for both ions. The Gibbs free energy (ΔG) for Pu(IV) extraction with both the ligands was found to be higher than that for Np(IV) extraction due to its higher extraction equilibrium constant (Table 1). This higher value of the ΔG suggests a

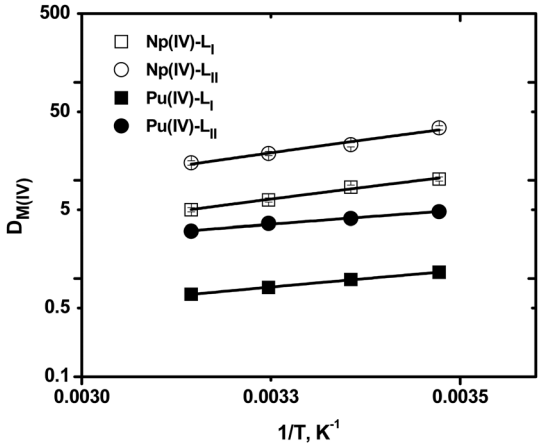

Fig. 3 Effect of temperature on the extraction of Np(IV) (open symbols) and Pu(IV) (closed symbols) with 0.1 mM $\mathbf{L_I}$ (squares)/$\mathbf{L_{II}}$ (circles) for Np(IV); and 0.01 mM $\mathbf{L_I}$ (squares)/$\mathbf{L_{II}}$ (circles) for Pu(IV) at 3 M HNO_3.

Table 1 Thermodynamic parameters for the extraction of Np(IV) and Pu(IV) by $\mathbf{L_I}$/$\mathbf{L_{II}}$ in 5% IDA + *n*-dodecane from 3 M HNO_3 at 298 K

Ligand	ΔG (kJ mol^{-1})	ΔH_0 (kJ mol^{-1})	$T\Delta S$ (kJ mol^{-1})	$\log K_{ex}'$
Np(IV)				
$\mathbf{L_I}$	−27.14 ± 0.06	−18.76 ± 1.17	8.38 ± 0.50	4.76 ± 0.01
$\mathbf{L_{II}}$	−29.62 ± 0.09	−20.53 ± 0.79	9.09 ± 0.24	5.19 ± 0.15
Pu(IV)				
$\mathbf{L_I}$	−40.40 ± 0.08	−11.29 ± 0.85	29.11 ± 0.39	7.08 ± 0.04
$\mathbf{L_{II}}$	−40.62 ± 0.10	−13.25 ± 0.29	27.37 ± 0.21	7.12 ± 0.18

stronger interaction of Pu(IV) with the ligands. The enthalpy contribution to the overall ΔG value is small for the extraction of Pu(IV) as compared with Np(IV) for both the ligands, whereas the reverse is true for the ΔS value. The higher contribution of ΔS in the case of Pu(IV) may be attributed to the release of coordinated water molecules from the primary and secondary hydration spheres and the 'distortion' created in the organic phase due the dissolution of the extracted complex, both adding to the entropy increase.

Back extraction studies

The back extraction of the tetravalent actinides Np(IV) and Pu(IV) by adjusting the acidity is difficult, hence aqueous complexing agents such as oxalic acid and HEDTA (hydroxyethyl ethylenediamine triacetic acid) were used.[22] The organic phase with extracted M(IV) was equilibrated with an aqueous phase containing 0.1 M HEDTA or 0.5 M oxalic acid in 0.05 M HNO_3. The quantitative back extraction of the tetravalent actinides Np(IV) and Pu(IV) could be achieved by 0.1 M HEDTA in 0.05 M HNO_3 compared with the 0.5 M oxalic acid in 0.05 M HNO_3 (Table 2).

Radiolytic stability studies

The liquid–liquid extraction process employed in the nuclear industry is always accompanied by the associated irradiation dose. It is desirable to have a good radiolytic stability of the extraction system. Therefore, the solvent system was irradiated with ^{60}Co to a cumulative dose of 300 kGy. Subsequently, the extraction of the M(IV) was done with the irradiated solvents from 3 M HNO_3 solution. The $D_{M(IV)}$ values decreased drastically upon irradiation, suggesting the poor radiation stability of the present systems at higher irradiation doses (Table 3).

DFT studies

Structural parameters. The minimum energy structures of the complexes of Np^{4+} towards the dendrimer ligands of generations 1 and 2 ($\mathbf{L_I}$ and $\mathbf{L_{II}}$) are displayed in Fig. 4. An analogous exercise was done for Pu^{4+} and the optimized structures are given in the ESI† (Fig. S5). In Fig. 4a, the Np^{4+} ion is coordinated to two DGA units and four monodentate nitrate ions leading to a deca-coordinated metal ion, whereas in Fig. 4b, the Np^{4+} ion is coordinated to one DGA unit and four nitrate ions (two monodentate and two bidentate) leading to a nona-coordinated metal ion. The calculated structural parameters for the Np^{4+} ion complexes are presented in Table 4 while those for the Pu^{4+} complexes are given in the ESI† (Table S3). The Np–O bond length for both the amidic 'O' as well as the etheric 'O' is longer than that of the corresponding Np–O bond length of the upper rim complex. Further, the metal–oxygen bond distance with the amidic O is shorter than that with the ethereal O atom, indicating that the amidic O will give a stronger interaction than the ethereal O atom. It must be noted that the Np–O bond length with nitrate O is shorter than that with the amidic O. In addition, the Np–O bond distance with the monodentate nitrate ion is shorter than that with the bidentate nitrate ions. Concerning ligand $\mathbf{L_{II}}$, in Fig. 4c, the Np^{4+} ion is coordinated to two DGA units and four monodentate nitrate ions leading to a nona-coordinated metal ion, whereas in Fig. 4d, the Np^{4+} ion is coordinated to one DGA unit and four nitrate ions (three monodentate and one bidentate) leading to an octa-coordinated metal ion. Similar structural information was obtained for the Pu^{4+} complexes (Fig. S5 and Table S3, ESI†).

Thermodynamical free energy of complexation. The free energy for the complexation of the Np^{4+} ion with $\mathbf{L_I}$ and $\mathbf{L_{II}}$, respectively, both in the gas phase and the solution phase is presented in Table 5. The well-known COSMO solvation approach was used to simulate the solvent phase as it is able to predict the solvent phase properties quite accurately. The gas phase free energy was seen to be reduced considerably due to the dielectric screening of the solution phase. The gas phase binding energy of complexation for $\mathbf{L_{II}}$ was found to be higher than for $\mathbf{L_I}$. Further, the complexation energy was found to be higher for monodentate nitrate ion over bidentate nitrate ion. In the case of the solution phase, the binding energy of complexation for $\mathbf{L_I}$ was found to be higher than for $\mathbf{L_{II}}$ for monodentate nitrate, whereas, the opposite trend is seen in the case of bidentate nitrate. The Gibbs free energy of complexation for $\mathbf{L_{II}}$ was found to be higher than that for $\mathbf{L_I}$ as observed in the case of the binding energy. Further, the complexation free energy was found to be higher for monodentate nitrate ion over bidentate nitrate ion. In the case of the solution phase, the binding energy of complexation for $\mathbf{L_{II}}$ was found to be higher than for $\mathbf{L_I}$ for bidentate nitrate, whereas, the opposite trend was seen in the case of monodentate nitrate. Overall, the solution phase free energy of complexation of Np^{4+} for $\mathbf{L_{II}}$ was higher than that of $\mathbf{L_I}$. In order to compare the preferable complexation between Np^{4+} and Pu^{4+} ions, the binding energy of the Pu^{4+} ion with the $\mathbf{L_I}$ and $\mathbf{L_{II}}$ ligands in both the gas and solution phases was determined and the calculated results are listed in Table 5. The binding energy of the Pu^{4+} ion with the DGA groups of $\mathbf{L_I}$ and $\mathbf{L_{II}}$ in both the gas and solution phases was seen to be higher than that with the Np^{4+} ion as observed in the experiment.

Table 2 Back extraction (%) of Np(IV) and Pu(IV) using 0.1 M HEDTA and 0.5 M oxalic acid (OA) in 0.05 M HNO_3; organic phase: 0.1 mM $\mathbf{L_I}$/$\mathbf{L_{II}}$ in 5% IDA + *n*-dodecane; *T*: 298 K

	% Back extraction			
	Np		Pu	
Aqueous phase	$\mathbf{L_I}$	$\mathbf{L_{II}}$	$\mathbf{L_I}$	$\mathbf{L_{II}}$
HEDTA	>99.9	99.0	96.2	77.5
OA	70.9	5.24	71.9	16.5

Table 3 Effect of irradiation of the organic phase on the extraction efficiency of Np(IV) and Pu(IV) from 3 M HNO_3; organic phase: 0.1 mM $\mathbf{L_I}$/$\mathbf{L_{II}}$ in 5% IDA + *n*-dodecane; *T*: 298 K

	$D_{Np(IV)}$		$D_{Pu(IV)}$	
Dose (kGy)	$\mathbf{L_I}$	$\mathbf{L_{II}}$	$\mathbf{L_I}$	$\mathbf{L_{II}}$
0	8.49 ± 0.02	23.12 ± 0.45	68.38 ± 3.84	74.95 ± 4.28
300	0.13 ± 0.01	0.16 ± 0.01	0.14 ± 0.01	0.03 ($<10^{-3}$)

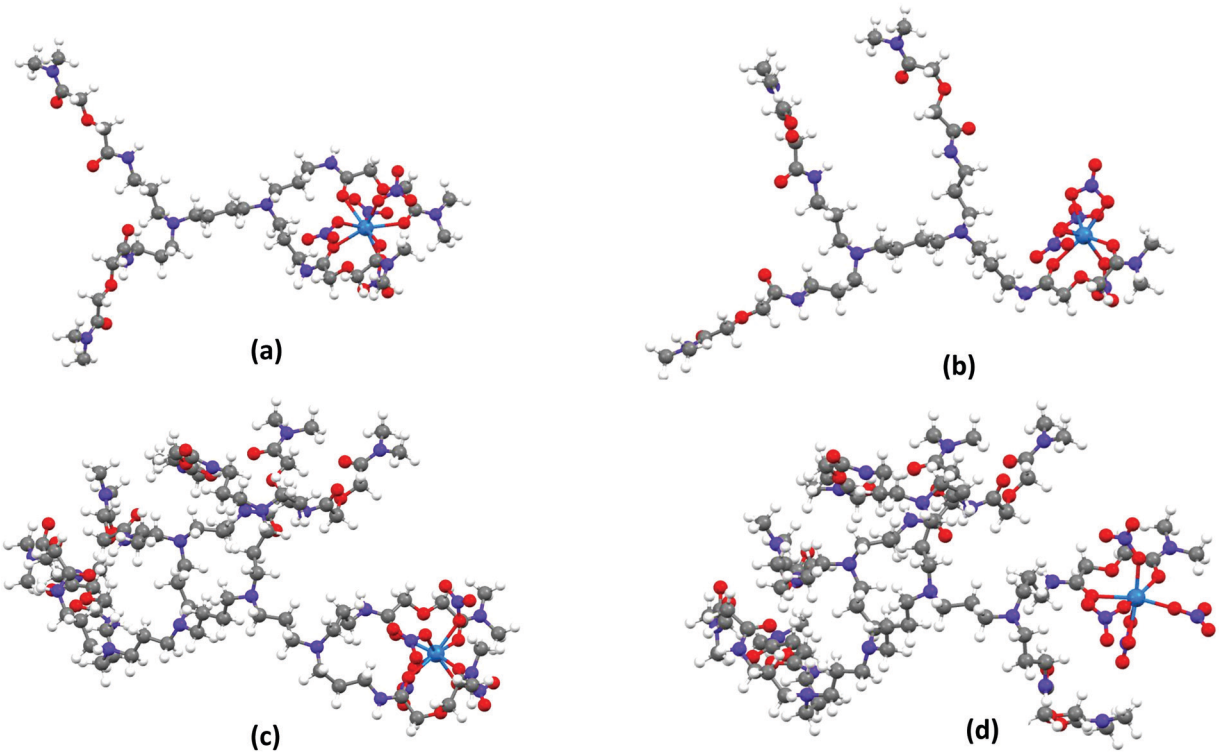

Fig. 4 Optimized structures of complexes of $\mathbf{L_I}$ and $\mathbf{L_{II}}$ with Np^{4+} at the B3LYP/SVP level of theory. (a) The Np^{4+} ion is coordinated to two DGA units and four monodentate nitrate ions; (b) the Np^{4+} ion is coordinated to one DGA unit and two monodentate and two bidentate nitrate ions; (c) the Np^{4+} ion is coordinated to two DGA units and four monodentate nitrate ions; and (d) the Np^{4+} ion is coordinated to one DGA unit and three monodentate and one bidentate nitrate ions. Grey: C, purple: N, red: O, white: H, blue: Np.

Table 4 Calculated structural parameters in Å at the B3LYP level of theory using the SVP basis set

System	Np–O (Å)	Np–O (Å)	Np–O (Å)
L_I			
Four nitrate ions as monodentate	O of C=O	Ether O	O of NO_3
	2.450, 2.405, 2.462, 2.434	2.861, 2.897	2.315, 2.328, 2.326, 2.349
Two nitrate ions as monodentate and two as bidentate	2.396, 2.413	2.774	2.244, 2.282, 2.408, 2.434, 2.405, 2.423
L_{II}			
Four nitrate ions as monodentate	O of C=O	Ether O	O of NO_3
	2.372, 2.377, 2.445, 2.547	3.769, 2.883	2.250, 2.270, 2.340, 2.431
Three nitrate ions as monodentate and one as bidentate	2.374, 2.402	2.733	2.179, 2.213, 2.260, 2.439, 2.444

Table 5 Calculated values of the interaction energy (kcal/mol) for Np^{4+} complexation in gas and *n*-dodecane phases at the B3LYP level of theory using the SVP basis set. The Pu^{4+} data are given in parentheses

	Binding energy		Gibbs free energy	
System	Gas	Dodecane	Gas	Dodecane
L_I				
Four nitrate ions as monodentate	−1758.26 (−1777.00)	−482.99 (−503.76)	−1680.39 (−1699.09)	−405.12 (−425.84)
Two nitrate ions as monodentate and two as bidentate	−1740.42 (−1766.10)	−469.25 (−497.14)	−1668.63 (−1694.15)	−397.48 (−425.18)
L_{II}				
Four nitrate ions as monodentate	−1767.61 (−1797.11)	−481.36 (−510.93)	−1685.03 (−1720.5)	−398.77 (−434.32)
Three nitrate ions as monodentate and one as bidentate	−1765.05 (−1788.02)	−480.51 (−505.82)	−1682.47 (−1712.1)	−405.80 (−431.87)

Table 6 Calculated charge and orbital population using NBO analysis in the gas phase at the B3LYP/SVP level of theory

System	Charge	s	p	d	f
$\mathbf{L_I}$					
Four nitrate ions as monodentate	1.581	4.19	11.97	11.10	4.14
Two nitrate ions as monodentate and two as bidentate	1.675	4.18	11.97	11.04	4.10
$\mathbf{L_{II}}$					
Four nitrate ions as monodentate	1.692	4.18	11.96	11.07	4.07
Three nitrate ions as monodentate and one as bidentate	1.808	4.16	11.96	11.00	4.05

Bonding analysis. To gain insight into the nature of the bonding in the complexes of actinide ions with the DGA-dendrimers $\mathbf{L_I}$ and $\mathbf{L_{II}}$, the charge on the metal ions and the atomic orbital population in the complexes were analyzed using the method of natural population analysis (NPA).[32] The calculated values are presented in Table 6. The substantial positive charge on the Np(IV) ion indicates an ion–dipole type of interaction in both cases. From NPA, it is revealed that there is a small extra orbital contribution to the inner s, and f subshells and a significant contribution in the d subshells of the metal ion, indicating that the interaction of the metal ion with the ligand has some covalent character. The d subshells were found to be more diffused than the s and f subshells. A similar bonding pattern was also observed with the Pu ion complexes (Table S4, ESI†).

Conclusions

The extraction of tetravalent actinide ions *viz.* Np^{4+} and Pu^{4+} was carried out from nitric acid solutions using the diglycolamide-functionalized poly(propylene imine) diaminobutane dendrimers $\mathbf{L_I}$ and $\mathbf{L_{II}}$ in a diluent mixture containing 5% isodecanol and 95% *n*-dodecane. The organic phase found to extract *ca.* 1% nitric acid from 3 M HNO_3 and the K_H values of the ligands $\mathbf{L_I}$ and $\mathbf{L_{II}}$ were determined to be 0.27 ($\pm$0.05) and 0.32 ($\pm$0.06). The extraction of the metal ions was found to be highly efficient as almost 90% or higher extraction of the metal ions was observed at 3 M HNO_3 using very dilute (1×10^{-4} M) ligand solutions. In general, the extraction with $\mathbf{L_{II}}$ was higher than that observed with $\mathbf{L_I}$ which was attributed to the higher hydrophobicity of the latter, while Pu(IV) extraction was higher than that of Np(IV), suggesting that the DGA-functionalized dendrimers to be one of the most efficient extractants of the tetravalent actinides reported so far.

The extracted species conformed to $M(NO_3)_4L$ for both Np(IV) and Pu(IV) with some contributions of $M(NO_3)_4{\cdot}2L$ for Pu(IV). As it was difficult to explain the bonding of the rather small tetravalent actinide ions (i.r. of Pu(IV): 0.96 Å; i.r. of Np(IV): 0.98 Å)[33] with so many DGA functional groups, it was attempted using DFT.

The gas phase as well as the solvent phase free energy of complexation for Np^{4+} as well as for Pu^{4+} ions, calculated using hybrid DFT, for $\mathbf{L_I}/\mathbf{L_{II}}$ was found to be always higher than that of the corresponding complexes as observed in the experiments. The free energy of complexation of Pu^{4+} ions with $\mathbf{L_I}$ and $\mathbf{L_{II}}$ in both the gas and solution phases was seen to be higher than that of with Np^{4+} ions as observed in the experiment. Different bonding analysis indicates the electrostatic and small covalent nature of the interactions between the metal ions and the chelating DGA-containing dendritic ligands.

Finally, the DGA-functionalized dendrimer ligands may be used for the extraction of tetra-valent ions from radioactive feeds where they may also extract the trivalent actinide ions albeit to a lower extent.[14] The extraction of U(VI) was however reported to be insignificant.

Experimental

Materials

DGA-functionalized poly(propylene imine) diaminobutane dendrimers $\mathbf{L_I}$ (Gen I) and $\mathbf{L_{II}}$ (Gen II) were prepared as described previously.[14] The purity of the ligands was checked with NMR spectroscopy and HR-MS. The diluents *n*-dodecane and isodecanol (IDA) (>99% purity) were obtained from Lancaster, UK, and SRL, Mumbai, respectively, and were used as obtained. The nitric acid solutions were prepared from Suprapur nitric Acid (Merck, Germany) and Milli Q water (Millipore) and were standardized using a conventional acid–base titrimetric method using AR grade NaOH (BDH) with phenolphthalein (Fluka, Switzerland) as the indicator.

Radiotracer

Pu (mainly ^{239}Pu) was purified by loading a known amount of Pu in 8 M HNO_3 at Dowex 1 × 8 anion exchange resin, followed by its elution with 0.5 M HNO_3. The purity of the eluted Pu sample was checked by alpha as well as gamma ray spectrometry. ^{239}Np was purified from a neutron irradiated uranyl nitrate hexa hydrate target by extracting it, after adjusting the Np valency to Np(IV) (*vide infra*), with 0.5 M TTA (2-thenoyltrifluoroacetone; Sigma-Aldrich) in xylene at 1 M HNO_3, and subsequent stripping by 8 M HNO_3. The aqueous solution was washed several times with xylene to remove any traces of the organic solvent. The purity of the ^{239}Np was checked by alpha as well as gamma ray spectrometry.

Oxidation state adjustment

Neptunium(IV). A solution of ferrous sulfamate solution (0.3 M) was freshly prepared by dissolving a known amount of iron powder (BDH) in sulfamic acid (Aldrich). The resultant Fe(II) sulfamate solution was used along with a few drops of hydroxylamine nitrate (1 M) as the reductant for the conversion of Np to its +4 state. The oxidation state of Np in the stock solution was confirmed intermittently by TTA extraction (ESI†).

Plutonium(IV). The oxidation state of Pu was also adjusted to the +4 state using a 0.05 M solution of $NaNO_2$ (Merck). Details of the oxidation state adjustment are given in the ESI.† Ammonium metavanadate (Aldrich) was used as the holding oxidant for Pu(IV) stabilization.

Distribution studies

Stock solutions of ligands $\mathbf{L_I}$ and $\mathbf{L_{II}}$ were prepared by dissolving a known amount of the ligands in 95% *n*-dodecane + 5% isodecanol. Appropriate dilutions were made as per the experimental requirements. The distribution ratios (D) of Np(IV) and Pu(IV) were measured by equilibrating equal volumes (usually 1 mL) of ligand solution in 5% IDA + *n*-dodecane with an aqueous solution containing ^{239}Np (*ca.* 10^{-12} M) and ^{239}Pu (*ca.* 10^{-6} M) in 5 mL stoppered glass centrifuge tubes for the required time in a constant temperature (25 ± 0.1 °C) water bath. The tubes were taken out and centrifuged at 3000 rpm for 5 min to get well separated aqueous and organic phases. Fixed volumes of both phases (50 μL for ^{239}Pu LSC and 100 μL for ^{239}Np γ-counting) were removed and assayed radiometrically. A toluene-based scintillator containing 10% di-(2-ethylhexyl)phosphoric acid (HD2EHP) was used for the α-counting of ^{239}Pu samples and a well type NaI(Tl) detector coupled with a multichannel analyzer was used for γ-counting of ^{239}Np. The D values were determined from the ratio of the activity per minute per unit volume of the organic phase to that in the aqueous phase. The extraction experiments were carried out in duplicate and the reported values are average values with an error of ≤5%.

ATR-FTIR studies

The ATR-FTIR of the $\mathbf{L_I}$/$\mathbf{L_{II}}$ dissolved in 5% isodecanol + 95% *n*-dodecane were recorded using a mono reflection ALPHA ATR-FTIR spectrophotometer (Bruker) with a monolithic diamond crystal. All spectra were obtained using a resolution of 4 cm^{-1} (wave number) under similar measurement conditions (3900–450 cm^{-1}). The presented ATR-FTIR is the average of at least 100 scans and used for the quantitative analysis of free and nitric acid bound $\mathbf{L_I}$/$\mathbf{L_{II}}$ complex in 5% isodecanol + 95% *n*-dodecane.

Temperature variation studies

The stock solutions of the ligands at an appropriate concentration and HNO_3 concentration were kept at the desired temperature for at least 30 min before the beginning of the temperature variation studies. The valency of Np and Pu was adjusted prior to the organic phase addition. Equal volumes of the aqueous and organic phases were added in 5 mL stoppered glass centrifuge tubes and equilibrated for 60 minutes at different temperatures using a temperature controlled (±0.1 °C) water bath. The tubes were taken out and quickly, to avoid any temperature variation, centrifuged at 3000 rpm for 1 min to get well separated aqueous and organic phases. The aqueous and organic phase activities were analyzed as described above.

Computational methodology

The structures of the free ligands $\mathbf{L_I}$ and $\mathbf{L_{II}}$ and their complexes with M^{4+} (M = Np or Pu) ion the in presence of nitrate ions were optimized using the Becke–Lee–Young–Parr (B3LYP) density functional[34] employing the split-valence plus polarization (SVP) basis set[35] as implemented in the TURBOMOLE suite of programs.[36] The scalar relativistic effective core potentials (ECP) were used for both the Np^{4+} and Pu^{4+} ions, where 60 electrons were kept in the core for Np and Pu.[37] The quartet spin state was used during the computation of structure and energy. Optimization was performed without any symmetry restrictions. The free energy was computed at 298.15 K using the B3LYP functional.[34] The hybrid B3LYP functional has been shown to be quite successful in predicting the thermodynamic properties of actinides.[38] The solvent phase was accounted for using a popular conductor like the screening model COSMO.[39] The dielectric constant of *n*-dodecane was taken to be 2. The model complexation reaction was used as follows:

$$pM^{4+}{}_{(aq)} + m{NO_3}^-{}_{(aq)} + nL_{(dodecane)} \rightarrow M_p(NO_3)_mL_{n(dodecane)} \quad (9)$$

where, M = Np or Pu.

The free energy of extraction, ΔG_{ext}, for the above complexation reaction was evaluated using our earlier reported thermodynamic procedure.[40]

Scalar relativistic effects for heavier lanthanide and actinide elements were included in the present computation using an earlier reported procedure.[41] Since there is a very small effect on the solvation energy between the gas phase and the solvent phase geometry,[42] the aqueous solvent effect was integrated by performing single point energy calculations using the optimized geometry obtained from the B3LYP level of theory employing the COSMO solvation model.

Conflicts of interest

There are no conflicts to declare.

Acknowledgements

The Computer division at BARC is acknowledged for providing the Anupam supercomputing facility. The authors (PKV, RBG and PKM) sincerely acknowledge Dr P. K. Pujari, Director, RC&IG and (SMA) Mr K. T. Shenoy, Associate Director, ChEG for continuous encouragement.

References

1 S. A. Ansari, P. N. Pathak, P. K. Mohapatra and V. K. Manchanda, *Chem. Rev.*, 2012, **112**, 1751–1772.

2 (*a*) J. N. Mathur, M. S. Murali and K. L. Nash, *Solvent Extr. Ion Exch.*, 2001, **19**, 357–390; (*b*) S. A. Ansari, P. Pathak, P. K. Mohapatra and V. K. Manchanda, *Sep. Purif. Rev.*, 2011, **40**, 43–76; (*c*) B. Christiansen, C. Apostolidis, R. Carlos, O. Courson, J.-P. Glatz, R. Malmbeck, G. Pagliosa,

K. Römer and D. Serrano-Purroy, *Radiochim. Acta*, 2004, **92**, 475–480.
3 M. I. Ojovan and W. E. Lee, *An Introduction to Nuclear Waste Immobilisation*, Elsevier, Amsterdam, 2005.
4 (*a*) Y. Sasaki, Y. Sugo, S. Suzuki and S. Tachimori, *Solvent Extr. Ion Exch.*, 2001, **19**, 91–103; (*b*) R. B. Gujar, S. A. Ansari, P. K. Mohapatra, M. S. Murali and V. K. Manchanda, *J. Radioanal. Nucl. Chem.*, 2010, **284**, 377–385; (*c*) S. A. Ansari, P. N. Pathak, V. K. Manchanda, M. Hussain, A. Prasad and V. S. Parmar, *Solvent Extr. Ion Exch.*, 2005, **23**, 463–479.
5 (*a*) W. Schulz and E. P. Horwitz, *Sep. Sci. Technol.*, 1988, **23**, 1191–1210; (*b*) E. P. Horwitz and D. G. Kalina, *Solvent Extr. Ion Exch.*, 1984, **2**, 179–200.
6 Y. Morita, J.-P. Glatz, M. Kubota, L. Koch, G. Pagliosa, K. Roemer and A. Nicholl, *Solvent Extr. Ion Exch.*, 1996, **14**, 385–400.
7 Y. Zhu and R. Jiao, *Nucl. Technol.*, 1994, **108**, 361–369.
8 (*a*) D. Serrano-Purroy, B. Christiansen, R. Malmbeck, J. P. Glatz and P. Baron, Partitioning of minor actinides from HLW using DIAMEX Process, Proc. Global, New Orleans, USA, 2003; (*b*) D. Serrano-Purroy, P. Baron, B. Christiansen, R. Malmbeck, C. Sorel and J.-P. Glatz, *Radiochim. Acta*, 2005, **93**, 351–355.
9 (*a*) G. Modolo, G. Asp, C. Schreinemachers and H. Vijgen, *Solvent Extr. Ion Exch.*, 2007, **25**, 703–721; (*b*) S. A. Ansari, D. R. Prabhu, R. B. Gujar, A. S. Kanekar, B. Rajeswari, M. J. Kulkarni, M. S. Murali, Y. Babu, V. Natarajan, S. Rajeswari, A. Suresh, R. Manivannan, M. P. Antony, T. G. Srinivasan and V. K. Manchanda, *Sep. Purif. Technol.*, 2009, **66**, 118–124; (*c*) R. B. Gujar, S. A. Ansari, D. R. Prabhu, P. N. Pathak, A. Sengupta, S. K. Thulasidas, P. K. Mohapatra and V. K. Manchanda, *Solvent Extr. Ion Exch.*, 2012, **30**, 156–170.
10 (*a*) P. K. Mohapatra, M. Iqbal, D. R. Raut, W. Verboom, J. Huskens and S. V. Godbole, *Dalton Trans.*, 2012, **41**, 360–363; (*b*) P. K. Mohapatra, A. Sengupta, M. Iqbal, J. Huskens and W. Verboom, *Inorg. Chem.*, 2013, **52**, 2533–2541.
11 (*a*) L. Wu, Y. Fang, Y. Jia, Y. Yang, J. Liao, N. Liu, X. Yang, W. Feng, J. Ming and L. Yuan, *Dalton Trans.*, 2014, **43**, 3835–3838; (*b*) C. Li, L. Wu, L. Chen, X. Yuan, Y. Cai, W. Feng, N. Liu, Y. Ren, A. Sengupta, M. S. Murali, P. K. Mohapatra, G. Tao, H. Zeng, S. Ding and L. Yuan, *Dalton Trans.*, 2016, **45**, 19299–19310.
12 A. Leoncini, P. K. Mohapatra, A. Bhattacharyya, D. R. Raut, A. Sengupta, P. K. Verma, N. Tiwari, D. Bhattacharyya, S. Jha, A. M. Wouda, J. Huskens and W. Verboom, *Dalton Trans.*, 2016, **45**, 2476–2484.
13 A. Leoncini, S. A. Ansari, P. K. Mohapatra, A. Boda, Sk. M. Ali, A. Sengupta, J. Huskens and W. Verboom, *Dalton Trans.*, 2017, **46**, 1431–1438.
14 A. Leoncini, S. A. Ansari, P. K. Mohapatra, A. Sengupta, J. Huskens and W. Verboom, *Dalton Trans.*, 2017, **46**, 501–508.
15 C. Madic, M. J. Hudson, J. O. Liljenzin, J.-P. Glatz, R. Nannicini, A. Facchini, Z. Kolarik and Z. R. Odoj, *New Partitioning Techniques for Minor Actinides*, EUR 19149, European Commission, Luxembourg, 2000, p. 59.
16 S. S. Kapoor, *Pramana*, 2002, **59**, 941–950.
17 A. Witze, *Nature*, 2014, **515**, 484–486.
18 A. Kumar, P. K. Mohapatra, P. N. Pathak and V. K. Manchanda, *Talanta*, 1997, **45**, 387–395.
19 S. Guoxin, L. Min, C. Yu, Y. Meilong and Y. Shaohong, *Solvent Extr. Ion Exch.*, 2010, **28**, 482–494.
20 J. Ravi, A. S. Suneesh, T. Prathibha, K. A. Venkatesan, M. P. Antony, T. G. Srinivasan and P. R. Vasudeva Rao, *Solvent Extr. Ion Exch.*, 2011, **29**, 86–105.
21 Z. Yoshida, S. G. Johnson, T. Kimura and J. R. Krsul, in *The Chemistry of the actinide and trans-actinide elements*, ed. L. R. Morss, N. M. Edelstein, J. Fuger and J. J. Katz, Springer, Dordrecht, The Netherlands, 3rd edn, 2006, vol. 2, p. 768.
22 B. Mahanty, A. Bhattacharyya, A. S. Kanekar and P. K. Mohapatra, *Solvent Extr. Ion Exch.*, 2020, **38**, 290–303.
23 W. J. Hamer and Y. C. Wu, *J. Phys. Chem. Ref. Data*, 1972, **1**, 1047–1100.
24 M. der Mar Marcos-Arroyo, M. K. Khoshkbarchi and J. H. Vera, *J. Solution Chem.*, 1996, **25**, 983–1000.
25 W. Davis Jr and H. De Bruin, *J. Inorg. Nucl. Chem.*, 1964, **26**, 1069–1083.
26 S. Bagawde, P. R. V. Rao, V. V. Ramakrishna and S. K. Patil, *J. Inorg. Nucl. Chem.*, 1978, **40**, 1913–1918.
27 T. Srinivasan, P. Vasudeva Rao and D. Sood, *Solvent Extr. Ion Exch.*, 1997, **15**, 15–31.
28 S. K. Patil, V. Ramakrishna, G. Avadhany and M. Ramaniah, *J. Inorg. Nucl. Chem.*, 1973, **35**, 2537–2545.
29 S. Bagawde, V. V. Ramakrishna and S. K. Patil, *J. Inorg. Nucl. Chem.*, 1976, **38**, 1339–1345.
30 S. K. Patil, V. V. Ramakrishna and M. V. Ramaniah, *Coord. Chem. Rev.*, 1978, **25**, 133–171.
31 J. Brothers, R. Hart and W. Mathers, *J. Inorg. Nucl. Chem.*, 1958, **7**, 85–93.
32 (*a*) A. E. Reed and F. Weinhold, *J. Chem. Phys.*, 1983, **78**, 4066–4073; (*b*) A. E. Reed, R. B. Weinstock and F. Weinhold, *J. Chem. Phys.*, 1985, **83**, 735–746; (*c*) A. E. Reed, L. A. Curtiss and F. Weinhold, *Chem. Rev.*, 1988, **88**, 899–926.
33 R. D. Shannon, *Acta Crystallogr., Sect. A: Cryst. Phys., Diffr., Theor. Gen. Crystallogr.*, 1976, **32**, 751–767.
34 (*a*) A. D. Becke, *J. Chem. Phys.*, 1993, **98**, 5648–5652; (*b*) C. Lee, W. Wang and R. G. Parr, *Phys. Rev. B: Condens. Matter Mater. Phys.*, 1988, **37**, 785–789.
35 A. Schaefer, H. Horn and R. J. Ahlrichs, *J. Chem. Phys.*, 1992, **97**, 2751–2777.
36 (*a*) R. Ahlrichs, M. Bär, M. Häser, H. Horn and C. Kölmel, *Chem. Phys. Lett.*, 1989, **162**, 165–169; (*b*) *TURBOMOLE V6.0 2009, a development of University of Karlsruhe and Forschungszentrum Karlsruhe GmbH*, TURBOMOLE GmbH, 1989–2007.
37 (*a*) M. Dolg, H. Stoll and H. Preuss, *J. Chem. Phys.*, 1989, **90**, 1730–1734; (*b*) W. Kuchle, M. Dolg, H. Stoll and H. Preuss, *J. Chem. Phys.*, 1994, **100**, 7535–7542; (*c*) X. Cao and M. Dolg, *THEOCHEM*, 2004, **673**, 203–209; (*d*) X. Cao and M. Dolg, *THEOCHEM*, 2002, **581**, 139–147.

38 A. Klamt, *J. Phys. Chem.*, 1995, **99**, 2224–2235.
39 G. A. Shamov, G. Schreckenbach and T. N. Vo, *Chem. – Eur. J.*, 2007, **13**, 4932–4947.
40 (*a*) Sk. M. Ali, J. M. Joshi, A. K. Singha Deb, A. Boda, K. T. Shenoy and S. K. Ghosh, *RSC Adv.*, 2014, **4**, 22911–22925; (*b*) Sk. M. Ali, *Comput. Theor. Chem.*, 2014, **1034**, 38–52; (*c*) Sk. M. Ali, *Eur. J. Inorg. Chem.*, 2014, 1533; (*d*) S. Pahan, A. Boda and Sk. M. Ali, *Theor. Chem. Acc.*, 2015, **134**, 41–57.
41 (*a*) C. Z. Wang, J. H. Lan, Q. Y. Wu, Y. L. Zhao, X. K. Wang, Z. F. Chai and W. Q. Shi, *Dalton Trans.*, 2014, **43**, 8713–8720; (*b*) J. P. Austin, M. Sundararajan, M. A. Vincent and I. H. Hiller, *Dalton Trans.*, 2009, 5902–5909; (*c*) D. Manna and T. K. Ghanty, *Phys. Chem. Chem. Phys.*, 2012, **14**, 11060–11069.
42 (*a*) G. A. Shamov and G. Schreckenbach, *J. Phys. Chem. A*, 2005, **109**, 10961–10974; (*b*) A. Boda, J. M. Joshi, Sk. M. Ali, K. T. Shenoy and S. K. Ghosh, *J. Mol. Model.*, 2012, **19**, 5277–5291; (*c*) A. Boda, Sk. M. Ali, K. T. Shenoy and S. K. Ghosh, *Sep. Sci. Technol.*, 2013, **48**, 2397–2409.